Cell, Vol. 92, 633–643, March 6, 1998, Copyright ©1998 by Cell Press

The VAB-1 Eph Receptor Tyrosine Kinase Functions in Neural and Epithelial Morphogenesis in *C. elegans*

Sean E. George,* Kristin Simokat,† Jeff Hardin,†‡ and Andrew D. Chisholm*§
*Department of Biology
Sinsheimer Laboratories
University of California
Santa Cruz, California 95064
†Program in Cellular and Molecular Biology
‡Department of Zoology
University of Wisconsin
Madison, Wisconsin 53706

Summary

Mutations in the *C. elegans vab-1* gene disrupt the coordinated movements of cells during two periods of embryogenesis. *vab-1* mutants are defective in the movement of neuroblasts during closure of the ventral gastrulation cleft and in the movements of epidermal cells during ventral enclosure of the embryo by the epidermis. We show that *vab-1* encodes a receptor tyrosine kinase of the Eph family. Disruption of the kinase domain of VAB-1 causes weak mutant phenotypes, indicating that VAB-1 may have both kinase-dependent and kinase-independent activities. VAB-1 is expressed in neurons during epidermal enclosure and is required in these cells for normal epidermal morphogenesis, demonstrating that cell–cell interactions are required between neurons and epidermal cells for epidermal morphogenesis.

Introduction

The shape of an organism is determined by the morphogenetic behavior of its cells. While we know much about the process of morphogenesis at the descriptive level and from experimental embryology and biochemistry, relatively little is known of the genetic mechanisms underlying morphogenetic movements (Bard, 1992). Many common types of morphogenetic movements involve epithelia, such as invagination and spreading (epiboly). One approach to understanding the molecular mechanisms underlying such movements is to use genetic analysis to identify mutants defective in such movements. Genetic analysis in *Drosophila melanogaster* has identified cell signaling pathways required for dorsal epidermal closure (Knust, 1997), including a JNK pathway that regulates cell shape changes in the leading edge (Glise et al., 1995; Riesgo-Escovar et al., 1996; Sluss et al., 1996), and TGFβ signaling pathways that may transmit signals to cells behind the leading edge. Another type of epithelial morphogenesis that has been analyzed genetically is ventral furrow invagination during *Drosophila* gastrulation. Genetic screens have identified two loci required for cell shape changes in gastrulation: the G_α subunit *concertina* (*cta)* (Parks and Wieschaus, 1991) and the novel secreted protein *folded gastrulation* (*fog)* (Costa et al., 1994). Thus, both these types of epithelial morphogenesis involve cell signaling, either via JNK and TGFβ pathways in epiboly or via *cta* and *fog* pathways in invagination.

The epidermis of the nematode *Caenorhabditis elegans* is a simple system in which to analyze epithelial morphogenesis. The epidermis, also known as hypodermis, begins as a set of cells born in the dorsal part of the embryo (Sulston et al., 1983) that forms an epithelial sheet. Ventral enclosure of the embryo by the epidermis occurs in two steps (Williams-Masson et al., 1997). Four anterior epidermal cells lead the migration of the epidermis to the ventral midline by extending actin-rich filopodia over substrate neurons. Once these leading cells have reached the midline, the remainder of the ventral midline appears to be enclosed by an actin-mediated purse-string mechanism. After enclosure is complete, circumferential constriction in the epidermis squeezes the embryo longitudinally (Priess and Hirsh, 1986).

To identify genes involved in epidermal morphogenesis, we have analyzed mutants in which morphogenesis is defective. *vab-1* mutants were originally isolated by Brenner (1974) based on their morphogenetic defects in head epidermis. Here, we show that *vab-1* is also required for cell movements following gastrulation and during ventral closure of the epidermis. We show that *vab-1* encodes an Eph receptor expressed in neuroblasts and neuronal cells and that *vab-1* function in these neuronal cells is required for epidermal morphogenesis. Our results provide an example of interactions between neuronal substrate cells and a migrating epithelial sheet in morphogenesis.

Results

vab-1 Mutants are Defective in Morphogenesis

The most striking defect of *vab-1* mutant larvae is the deformation of head epidermis, the "Notched head" phenotype (Brenner, 1974; Figures 1A and 1B); epidermal morphogenesis is often also abnormal in the tail region (Figure 1B). Morphology of the body is normal in most *vab-1* mutants. The phenotypes caused by *vab-1* alleles are incompletely penetrant and variably expressed, hence the gene name *vab* (variable *ab*normal). The number of head epidermal cells and nuclei is normal in Notched head *vab-1* mutants, as determined by Nomarski microscopy and expression of epidermal markers (data not shown), indicating that the Notched head phenotype results specifically from abnormal morphogenesis of head epidermal syncytia (Figures 1C and 1D).

Seventeen recessive zygotic *vab-1* mutant alleles have been isolated by various workers (see Experimental Procedures). We classified *vab-1* alleles as strong, intermediate, or weak, based on the penetrance of mutant phenotypes (Table 1); most animals mutant for strong *vab-1* alleles arrest during embryogenesis due to defects in epidermal enclosure (see below), whereas weak *vab-1* mutants are almost fully viable. By genetic and molecular criteria (Tables 1 and 2), the strong *vab-1* alleles cause complete loss of function.

§To whom correspondence should be addressed.

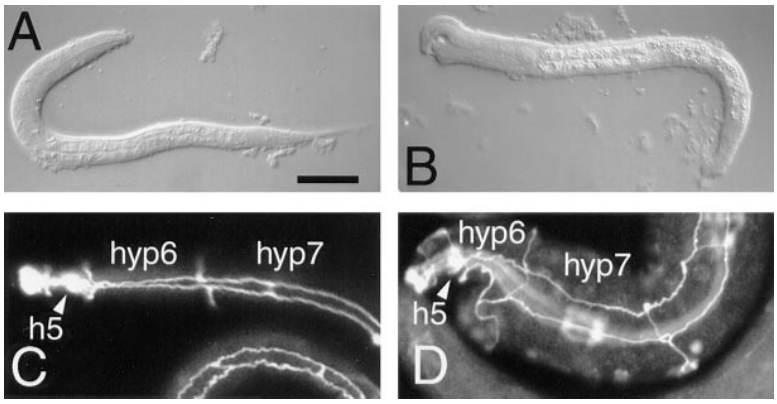

Figure 1. Morphogenetic Phenotypes of *vab-1* Mutant Larvae

(A) Wild-type first stage (L1) larva. Anterior is to the left, and dorsal is up. Bar, 20 μm.

(B) Abnormal Notched head and abnormal tail morphogenesis of *vab-1(e2027)* L1 larva.

(C) Wild-type L1 larva stained with the MH27 monoclonal antibody to show junctions between epidermal cells; the head epidermal syncytia hyp5 (h5), hyp6, and hyp7 are marked.

(D) *vab-1(dx14)* mutant L1 larva, MH27 staining, showing malformation of hyp5, hyp6, and hyp7 cells.

vab-1 Null Mutations Cause Variable Defects in Cell Movements following Gastrulation and during Embryonic Ventral Enclosure of the Epidermis

To determine the role of *vab-1* in embryonic development of the epidermis, we analyzed the embryogenesis of *vab-1* mutant embryos using conventional and four-dimensional Nomarski microscopy. We found that *vab-1* null mutant embryos are variably defective in the movements of neuroblast cells during closure of the ventral gastrulation cleft and in the migrations of epidermal cells during ventral enclosure of the epidermis. These defects in cell movements result in failure of enclosure of the embryo by epidermal cells, and such embryos arrest because internal cells leak out at the ventral midline. The variable phenotypes of *vab-1* null mutants can be described in terms of five phenotypic classes (Figure 2 legend).

Approximately 35% of *vab-1* null mutant animals displayed defects in cell movements following gastrulation. During normal *C. elegans* gastrulation, a ventral cleft is formed by the movement of endoderm, mesoderm, and germline precursors into the interior of the embryo; this cleft is gradually closed by the short-range lateral movements of many neuroblasts (Figures 2A and 2C) (Sulston et al., 1983). In 20% of *vab-1* embryos (phenotypic classes I and II), the ventral cleft is deeper than normal and remains for longer (Figure 2E); in 15% of embryos the cleft is of normal depth and lasts longer (class III). These phenotypes appear to result from delays in the

Table 1. Strength of *vab-1* Mutations and Molecular Lesions

Allele	Embryonic Arrest	Larval Arrest	Adult, Vab	Adult, Non-Vab	Wild-Type Sequence	Mutant Sequence	Predicted Effect
Strong							
e2027	58.2%	31.3%	8.9%	2.5%	—	74 bp deletion removing first 7 bp of exon 5	
e721	58.2%	29.3%	11.4%	1.0%	ND	ND	
dx14	56.1%	29.6%	9.5%	4.7%	—	deletion of exon 4, part of exon 5	
ju8	53.3%	32.5%	13.2%	0.8%	CAA	AAA	E62K
dx31	50.8%	33.2%	14.0%	2.0%		deletion of exons 1–4	
e1059	49.9%	36.0%	12.5%	1.4%	CAG	TAG	Q21amber
Intermediate							
tn2	30.3%	14.9%	33.4%	21.3%	TGG	TAG	W932amber
e856	19.9%	26.7%	45.0%	8.4%	GAG	AAG	E195K
e699	9.0%	20.9%	51.2%	19.8%	ACT	ATT	T63I
Weak							
e118	10.1%	8.6%	45.6%	35.8%	—	326 bp deletion in exon 10	
e2	10.2%	5.5%	31.4%	51.4%	GGA	GAA	G917E
ju63	9.2%	7.0%	52.1%	31.5%	CAG	TAG	W964amber
ju22	8.5%	6.4%	53.8%	31.2%	TGT	TTT	C966F
e1063	8.3%	6.6%	51.0%	34.0%	TGT	TAT	C966Y
e116	6.4%	17.5%	50.7%	25.3%	TGG	TGA	W921opal
e200	5.6%	3.1%	44.4%	46.7%	tttcag|AAG	tttcaa|AAG	exon 2 splice acceptor
e1029	5.9%	1.9%	45.7%	46.5%	ND	ND	

Mutant phenotypes were quantitated as described in Experimental Procedures. We classify *vab-1* mutations as strong (>50% lethality), intermediate (25%–50% lethality), or weak (<25% lethality). Most larval arrest animals arrested during L1 or L2 stages; some *vab-1* larvae rupture at the rectum. Some (<5%) adult animals showed egg-laying defects. Wild-type and mutant *vab-1* genomic DNA sequences are shown with the predicted effects on VAB-1 protein.

ND, not determined.

Table 2. The *vab-1* Null Phenotype Is a Variable Defect in Morphogenesis

Parental Genotype (n)	Arrest at or before 2-Fold	Arrest Later Than 2-Fold	Hatched, Abnormal Head or Tail	Hatched, Normal Head and Tail
vab-1(133)	18.0% (24)	23.3% (31)	58.6% (78)	0% (0)
vab-1/+ (152)	8.5% (13)	7.8% (12)	11.2% (17)	72% (110)
vab-1/+ × *ccDf4*/+ (81)	8.6% (7)	5% (4)	11.1% (9)	75.3% (61)
ccDf4/+ × *maDf4*/+ (105)	12.3% (13)	7.6% (8)	3.8% (4)	76.2% (80)

Arrest stages of *vab-1* mutants were scored as described in Experimental Procedures. Arrest at or before 2-fold stages corresponds to phenotypic Classes I-III and some Class IV phenotypes, arrest later than 2-fold corresponds to a subset of Class IV phenotypes, embryos that hatch correspond to Class V. Data for the strong *vab-1* allele *e2027* are shown; similar results were obtained for other strong *vab-1* alleles. Similar ranges of phenotypes are seen in progeny from homozygous *vab-1(e2027)* mothers and in one quarter of the progeny of *vab-1(e2027)*/+ mothers, indicating that there is no maternal effect for *vab-1*. The range of phenotypes of *vab-1(e2027)*, *vab-1(e2027)/Df*, and *Df/Df* animals are similar, consistent with *vab-1(e2027)* being a null mutation.

lateral movements of the neuroblasts that normally close the gastrulation cleft. Thus, *vab-1* function is required for neuroblast movements following gastrulation.

Approximately 35% of *vab-1* null mutant embryos displayed severe defects in cell movements during the process of epidermal enclosure. During ventral enclosure of the epidermis in wild-type embryos, leading cells of the epidermis migrate over neurons, from lateral positions to the ventral midline (Figures 2B and 2D) (Williams-Masson et al., 1997). The epidermal leading edge cells fail to migrate or migrate more slowly than normal in *vab-1* animals (phenotypic class I: Figure 2F), or they migrate to the ventral midline and fail to form junctions correctly (class II). The leading cells in class I and II embryos often send actin-rich processes to abnormally anterior regions, as determined by phalloidin staining (data not shown), and migrate to abnormally anterior positions (Figure 2F). As a result, ventral closure is incomplete, and internal cells ooze through a hole in the ventral midline of the epidermis when elongation begins, resulting in rupture and arrest of the embryo. In other embryos (class III) the leading cells meet up normally, but internal cells ooze from the region of the posterior leading cells after elongation (Figure 2I), suggesting that the cells do not properly connect with their partners. In 65% of *vab-1* embryos, closure of the gastrulation cleft appears normal, and the embryos elongate to the 1.5-fold or 2-fold stage (classes IV and V); about one-third of these embryos rupture along the ventral midline at the 2-fold stage or later (Figure 2J), indicating a late defect in ventral enclosure; and the remaining two-thirds do not rupture (class V; data not shown). The phenotype of class IV embryos, in which closure of the ventral gastrulation cleft is normal but epidermal enclosure is defective, suggests that the ventral enclosure defects in *vab-1* embryos are not merely a consequence of the defects in ventral cleft closure.

In *vab-1* embryos, internal organs and tissues differentiate normally, as judged by Nomarski microscopy. Several markers of neuronal and epidermal cell fates were examined and showed normal expression in *vab-1* mutants (data not shown). Thus, the morphogenetic defects in *vab-1* embryos do not appear to be due to improper specification of neural or epidermal fates.

vab-1 Encodes an Eph Receptor Protein-Tyrosine Kinase

We cloned *vab-1* using genetic mapping and transformation rescue. We mapped *vab-1* close to the right of *hlh-1*, tested genomic DNA clones from this region (Figure 3A) for their ability to rescue Vab-1 phenotypes in transgenic lines, and found that the cosmid M03A1 fully rescued *vab-1(e2027)* mutant phenotypes. Genomic sequence available from the *C. elegans* genome consortium predicted a gene from this cosmid that could encode a receptor protein-tyrosine kinase (RPTK) of the Eph subfamily. This RPTK gene is mutated in *vab-1* mutants (see below), establishing that this gene is *vab-1*. *vab-1* produces a 4 kb transcript expressed throughout development (data not shown). We determined the cDNA sequence corresponding to this *vab-1* transcript as described in Experimental Procedures.

The predicted VAB-1 protein (Figure 4A) is most similar to Eph-related RPTKs, recently renamed Eph receptors (Eph Nomenclature Committee, 1997). The Eph receptor subfamily is the largest subfamily of RPTKs (Orioli and Klein, 1997). EphA receptors bind GPI-linked ephrin ligands, and EphB receptors bind transmembrane ephrins (Gale et al., 1996); VAB-1 shows equal sequence similarity to EphA and EphB subclasses. VAB-1 contains all hallmark features of Eph receptors (Figures 3B and 3C), including in its extracellular domain an N-terminal globular domain with weak similarity to immunoglobulin domains (O'Bryan et al., 1991), a cysteine rich domain, in which the positions of the cysteine residues are highly conserved among Eph family members, and two fibronectin type III repeats. The intracellular domain of VAB-1 contains the juxtamembrane motif Y(I/V)DPXTYEDP found in all vertebrate Eph receptors and a tyrosine kinase catalytic domain most similar (59% identical) to that of human EphA3/Hek and between 51% and 58% identical to those of other Eph receptors (Figure 3E). Unlike other Eph receptor kinase domains, the VAB-1 kinase domain contains an insert sequence (A719-E743) between subdomains I and II.

Mutations in the VAB-1 Extracellular Domain Cause Strong or Intermediate Mutant Phenotypes

To identify functionally important parts of the VAB-1 protein, we determined the molecular lesions of *vab-1* mutant DNAs (Table 1). Several of the strong alleles had lesions consistent with their genetic behavior as null mutations. Three strong alleles, *dx14*, *dx31*, and *e2027*, cause deletions of sequences encoding parts of the extracellular domain (Figure 3A), and *e1059* is an amber stop in the signal peptide. One strong and two intermediate alleles cause missense alterations in the extracellular

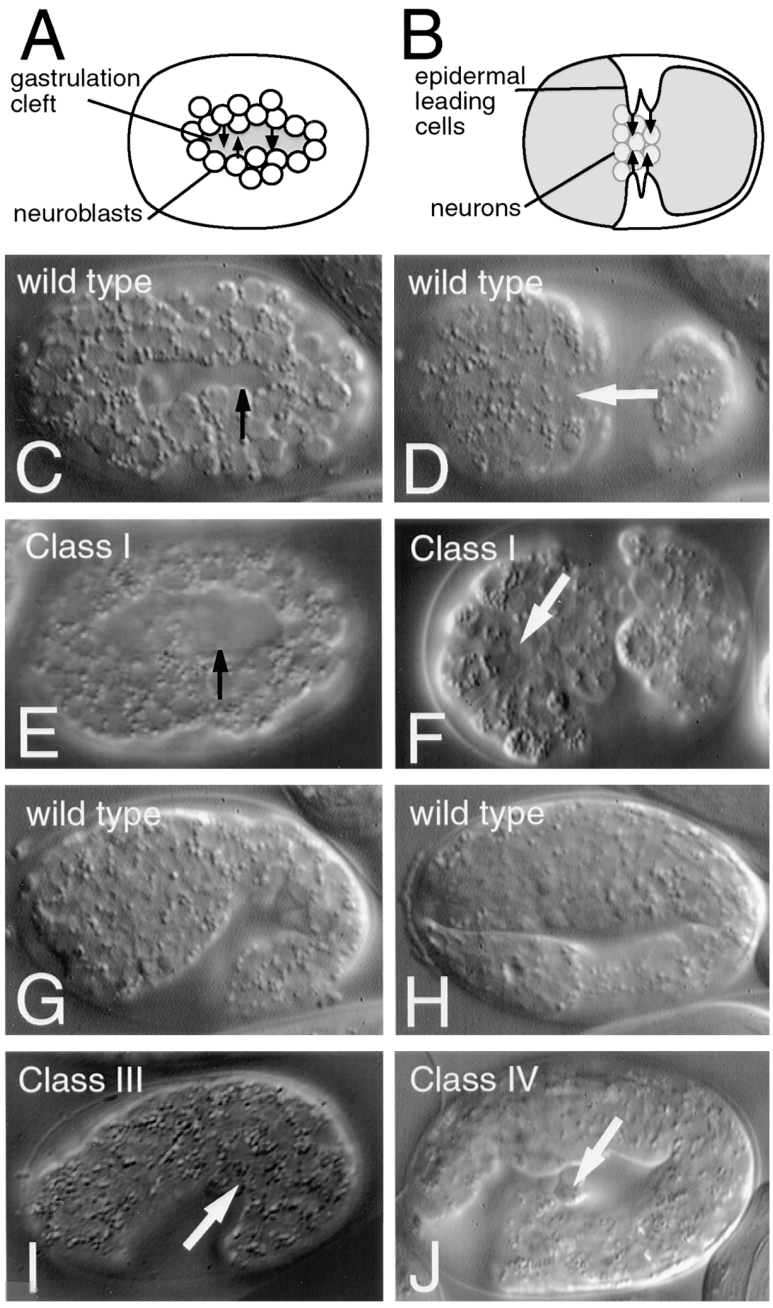

Figure 2. Cell Movement Defects following Gastrulation and during Ventral Closure in *vab-1* Embryos

In wild-type embryos the gastrulation cleft (A and C) is normally 1–2 μm deep and closes 230–290 min postfertilization; epidermal enclosure (B and D) occurs between 310–340 min. (C–F), ventral Nomarski views, anterior to left. Bar, 15 μm. (G–H), lateral views.

vab-1 class I phenotype (~14% of animals): embryo is rounded, double ventral gastrulation cleft forms single cleft (arrow in [E]) 4–5 μm deep that persists throughout enclosure. Ventral closure fails early (F): leading cells (arrow) fail to migrate or migrate slowly. In class I embryos the ventral pocket attempts to form, and the embryos display muscular twitching. The class II phenotype (~5% of animals, data not shown) is similar, only weaker. (G and H) Wild-type comma stage and 2-fold stage embryos. Animals displaying a class III phenotype (~15% of animals) show a transient 1–2 μm deep cleft, similar to wild-type but persisting approximately 30 min longer. The leading edge cells zip up normally, and the ventral pocket forms. The embryo oozes from the region of the posterior leading edge after elongation begins (arrow, [I]). Class IV animals (~23% of animals) initially appear normal and elongate to the 1.5-fold or 2-fold stage, then ooze along the ventral midline in the head or tail (arrow, [J]). Class V embryos (~43% of animals; data not shown) show no embryonic abnormality and hatch. Some class III, IV, and V embryos have enlarged buccal cavities and develop a Notched head.

domain and might define functionally important residues in Eph receptors. The strong allele *ju8* and the intermediate allele *e699* affect residues (E62K and T63I, respectively) in the N-terminal globular domain, and the *e856* mutation affects the cysteine-rich domain (Figure 3D); these domains have been implicated in ephrin–Eph receptor interactions (Labrador et al., 1997).

Mutations in the VAB-1 Kinase Domain Cause Weak Mutant Phenotypes

Seven *vab-1* mutations disrupt the kinase domain of VAB-1 (Figure 3E) and are likely to cause severe loss of kinase activity (see Discussion). Strikingly, six of these seven alleles cause weak mutant phenotypes. The weak alleles *e2*, *e1063*, and *ju22* cause missense alterations of conserved residues that function to stabilize the structure of other kinase domains (Hubbard et al., 1994). Three weak alleles should truncate the kinase domain: *ju63* and *e116* cause stop codons, and *e118* is a deletion of the C-terminal 202 residues of VAB-1. One allele, *tn2*, causes a stop codon in kinase subdomain IX yet causes an intermediate mutant phenotype; it is unclear why the *tn2* phenotype is stronger than those of the other kinase domain alleles. The above mutations would be predicted to abolish catalytic activity of VAB-1, yet none appears to cause complete loss of *vab-1* function, suggesting that VAB-1 may possess both kinase-dependent and kinase-independent functions.

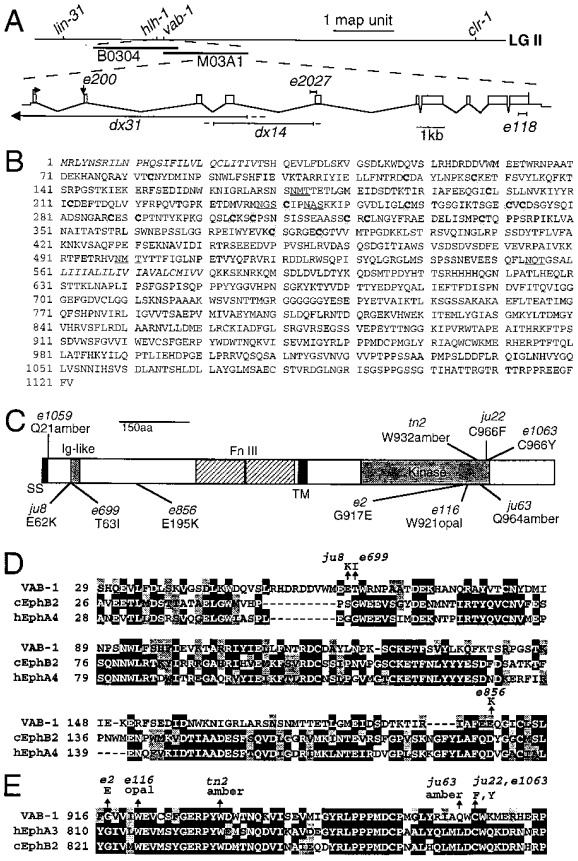

Figure 3. Molecular Cloning and Sequence Analysis of *vab-1*

(A) Genetic and physical maps of the *vab-1* region and structure of the *vab-1* transcription unit. Genetic mapping placed *vab-1* 0.07 map units to the right of *hlh-1*. Cosmid clones were mapped by the *C. elegans* genome project. B0304 contains *hlh-1*; M03A1 contains *vab-1*. The position of the intron between exons 2 and 3 is conserved between *vab-1* and chicken EphB2 (Connor and Pasquale, 1995), and the position of the intron between exons 6 and 7 is conserved between *vab-1*, chicken EphB2, and rat EphA5 (Maisonpierre et al., 1993), suggesting that these genes might share a common ancestor. Locations of the deletions *dx14*, *dx31*, *e2027*, *e118*, and the splice site mutation *e200* are shown.

(B) Sequence of the predicted VAB-1 protein. The signal sequence (residues 1-28) and transmembrane domain (residues 559-581) are italicized. Potential N-linked glycosylation sites (NX[T/S]) are underlined. The conserved cysteines in the cysteine-rich domain are in boldface and shaded.

(C) Domains of VAB-1 and locations of point mutations. SS, signal sequence; TM, transmembrane domain.

(D) Alignment of the VAB-1 N-terminal globular domain and part of the cysteine-rich-domain with those of the closest vertebrate EphA and EphB receptors. The VAB-1 extracellular domain (residues 55-550) is most similar (27% identity, 42% similarity) to chicken EphB2/Cek5 (Pasquale, 1991); within the EphA subfamily the extracellular domain of human EphA4/Hek8 (Fox et al., 1995) is most similar to VAB-1 (27% identity, 41% similarity). Sequences were aligned using ClustalW; identities are in black and conserved residues in gray. *ju8*, which changes a glutamate to a lysine (charge reversal), and the intermediate allele *e699*, which changes a polar residue (threonine) to a nonpolar residue (isoleucine) affect a poorly conserved part of the N-terminal globular domain. The intermediate allele *e856* changes a glutamate to a lysine; the equivalent residue is aspartate (negatively charged) in most vertebrate Eph receptors.

(E) Alignment of VAB-1 kinase subdomains IX-XI with the most similar vertebrate EphA and EphB kinase domains and location of *vab-1* kinase domain mutations. The VAB-1 kinase domain (residues 665-991) is most similar (59% identity, 72% similarity) to that of human EphA3/Hek (Wicks et al., 1992); the EphB with highest similarity to VAB-1 in the kinase domain is chicken EphB2/Cek5 (58% identity, 72% similarity).

vab-1 Reporter Constructs Are Widely Expressed in Early Embryos but Only in Nonepidermal Cells during Ventral Enclosure

To determine the pattern of expression of *vab-1*, we used reporter constructs containing translational fusions of the *vab-1* locus to green fluorescent protein (GFP; see Experimental Procedures). Such *vab-1*::GFP constructs fully rescued *vab-1(e2027)* mutant phenotypes, indicating that these constructs reflect the endogenous *vab-1* expression pattern. Expression from one such construct, *juIs24*, was analyzed in detail.

VAB-1::GFP was expressed in many cells during late gastrulation; based on their positions these cells include the neuroblasts whose movement is defective in *vab-1* mutants (Figure 4A) and may also include some epidermal precursors. During ventral enclosure of the epidermis, VAB-1::GFP was expressed in clusters of cells of the head and tail regions (Figures 4B–4F). In the head region, VAB-1::GFP was expressed in clusters of presumptive neuronal cells. Early in enclosure these cells appear to lie beneath the epidermal leading cells (Figures 4C and 4D); later in enclosure, the VAB-1–expressing cells lie anterior to the leading cells (Figure 4E). VAB-1::GFP was not detectably expressed in the epidermal leading cells at any stage during ventral enclosure. In the posterior of the embryo, VAB-1::GFP was expressed in several cells, including QV5 and the ventral hyp7 cells posterior to the rectum (data not shown); VAB-1::GFP was also expressed in several pharyngeal cells (Figure 4G). In late embryogenesis and throughout larval and adult development, VAB-1::GFP was localized to the axons of many neurons throughout the nervous system (Figures 4G and 4H). Thus, in most stages following gastrulation, VAB-1::GFP is widely expressed in the developing nervous system. Expression of VAB-1::GFP in the larval nervous system suggested that *vab-1* might function in neural development; although *vab-1* mutants do not display obvious behavioral defects, we have found that *vab-1* mutants display defects in axonal outgrowth and fasciculation (S. E. G. and A. D. C., unpublished data).

vab-1 Function Is Required in Nonepidermal Cells for Epidermal Morphogenesis

The expression of VAB-1::GFP reporter constructs in nonepidermal cells during epidermal enclosure led us to ask whether the epidermal morphogenetic defects in *vab-1* mutants are due to a requirement for *vab-1* function in neurons. We used genetic mosaic analysis (Herman, 1995) to determine in which cells *vab-1* is necessary for normal morphogenesis. Because genetic mosaics could not be identified during embryogenesis, we analyzed viable *vab-1* genetic mosaics. We identified 83 *vab-1* genetic mosaics, 56 of which displayed morphogenetic defects in head epidermis (the Vab phenotype). All such Vab mosaics proved to have lost *vab-1* within the AB lineage, which generates head epidermal

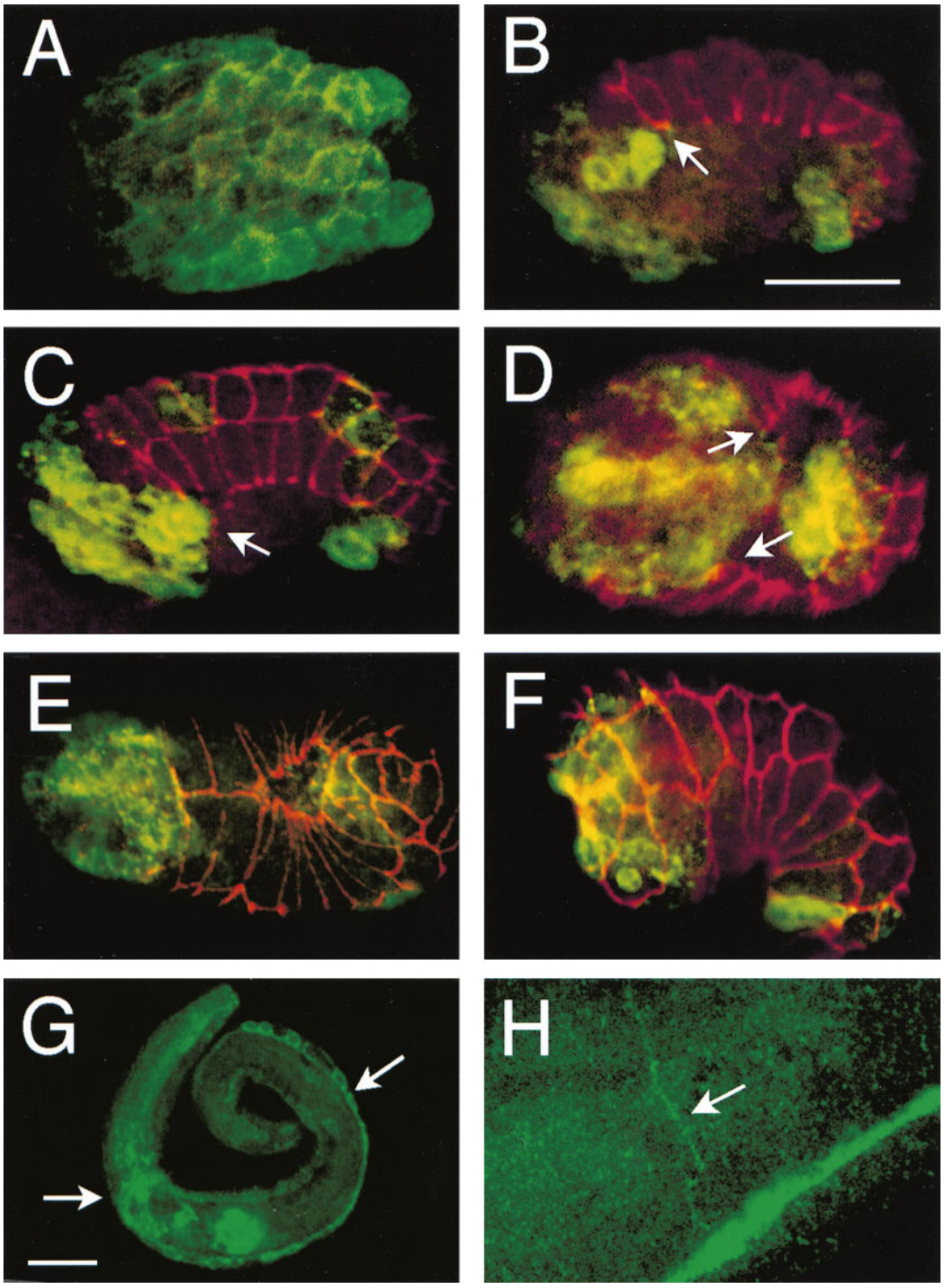

Figure 4. Expression Pattern of *vab-1* Reporter Constructs

Confocal images of VAB-1::GFP expression from the *juIs24* transgene (visualized using anti-GFP antibodies [green]) and epidermal cell junctions (MH27 antigen [red]). Bars, 15 μm. (A) VAB-1::GFP expression in postgastrulation embryo (~200–250 min). Ventral view. Not all VAB-1–expressing cells have been identified at this stage; based on position most of the cells are neuroblasts. Some epidermal precursors may also express VAB-1::GFP. (B and C) Beginning of ventral closure, ventrolateral and ventral views (D). Later in ventral closure, leading epidermal cells are marked (arrows). (E) Midventral closure; leading cells have met at ventral midline, ventral view; ventral pocket has not yet closed. (F) Completed ventral enclosure (comma stage). (G) L1 larval animal showing expression of VAB-1::GFP (*juIs33* transgene) in the nervous system; nerve ring and ventral nerve cord are arrowed. Strong expression is also seen in the procorpus and terminal bulb of the pharynx. (H) Expression of VAB-1::GFP in axons in late larval animal; lateral view, close-up of expression in D neuron axon commissure (arrowed) and ventral cord.

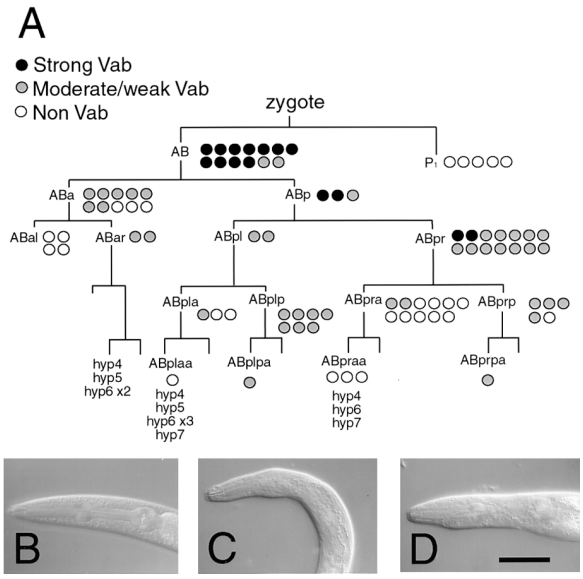

Figure 5. Mosaic Analysis of *vab-1*

(A) Partial lineage of *C. elegans* showing points at which arrays were lost in *vab-1* mosaic animals. The origin of the main head epidermal syncytia (hyp4, hyp5, hyp6, and anterior of hyp7) is shown. Black circle, strong head morphogenetic defect; gray circle, moderate or weak morphogenetic defect (Figures 6C and 6D). Open circle, wild-type morphology. (B) Wild-type (N2) head morphology. (C and D) Vab phenotypes resulting from losses of *vab-1* function outside of the epidermis. (C) Head region of typical ABprp mosaic, L4 stage, displaying moderate Vab phenotype. (D) Typical ABplp mosaic displaying moderate Vab phenotype. Bar, 20 μm.

cells, neuronal cells, and neuronal support cells (Figure 5A). In general, only early losses (in AB or ABp) of *vab-1* function caused strong morphogenetic defects, suggesting that *vab-1* functions in many AB-derived cells. Five losses of *vab-1* function outside the AB lineage did not cause morphological defects (Figure 5A).

The early focus of *vab-1* function in the AB lineage might reflect a requirement for *vab-1* in many epidermal cells, in many nonepidermal cells, or both. To determine whether *vab-1* was required in epidermal or nonepidermal cells, we identified mosaics in which *vab-1* had been lost from precursors at the AB^8 stage or later; at this stage three precursors (ABarp, ABpra, and Abpla) generate the head epidermal cells hyp4, hyp5, and hyp6. Three of 18 mosaic animals in which *vab-1* was lost in epidermal precursors (in ABpla, ABplaa, Abpra, or ABpraa) displayed Vab phenotypes. By contrast, 12 of 14 mosaic animals in which *vab-1* had been lost only from nonepidermal precursors (ABplp, ABplpa, ABprp, and ABprpa) displayed Vab phenotypes (Figures 5B and 5C). Our data clearly show that losses of *vab-1* function in neuronal lineages cause non–cell-autonomous defects in epidermal morphogenesis, consistent with our data showing that VAB-1::GFP is mostly expressed in neurons from the ventral enclosure stage onward. However, we cannot exclude the possibility that *vab-1* has additional cell-autonomous roles in the epidermal cells.

Discussion

We show here that *vab-1*, which functions in epidermal morphogenesis in *C. elegans*, encodes an Eph receptor tyrosine kinase. The phenotypes of null and kinase domain mutations in VAB-1 suggest that the VAB-1 RTK has both kinase-dependent and kinase-independent functions. Our analysis of *vab-1* mutant phenotypes, expression pattern, and genetic mosaics suggests that *vab-1* functions in neuronal cells to regulate normal morphogenesis of the epidermis.

Evolutionary Conservation of Eph Signaling Pathways

VAB-1 is most similar to receptor tyrosine kinases of the Eph subfamily. Eph receptors were first isolated from vertebrates by homology in the kinase domain (Hirai et al., 1987) and are the largest subfamily of RPTK (Orioli and Klein, 1997). Previously, Eph receptors have only been reported from vertebrates. Our findings show that the Eph receptor family is ancient and likely to be conserved among all animals.

Eph receptors bind membrane-bound protein ligands, recently renamed ephrins (Eph Nomenclature Committee, 1997). Ephrins are either membrane-anchored in cell membranes via glycosylphosphatidylinositol (GPI) anchors (ephrin-As) or are integral membrane proteins (ephrin-Bs). Eph receptors can be grouped into two subclasses: the EphA receptors, which bind ephrin-A ligands, and the EphB receptors, which bind transmembrane ephrin-B ligands (Gale et al., 1996). VAB-1 is equally similar in sequence to EphA and EphB receptors and thus may be similar to a common ancestor of the two vertebrate subclasses. We have also identified ephrin-related genes in the *C. elegans* genomic sequence (A. D. C. and S. E. G., unpublished data), indicating that potential ligands for VAB-1 exist in *C. elegans* and thus that ephrin signaling pathways may be conserved between nematodes and vertebrates.

VAB-1 Might Participate in Forward and Reverse Signaling

Vertebrate Eph receptors may participate in both kinase-dependent "forward" signaling and in kinase-independent "reverse" signaling. For example, deletion of the kinase domain of murine Nuk/EphB2 did not affect its function in axonal guidance in the anterior commissure (Henkemeyer et al., 1996). EphB2 is not expressed on anterior commissure axons but on substrate cells over which the axons navigate. A transmembrane ligand for EphB2, ephrin-B1/LERK-2, is expressed on anterior commissure axons, and EphB2 binding to ephrin-Bs can induce phosphorylation of tyrosines on the intracellular domain of the ephrin-B, thus potentially activating a signaling cascade in the ligand-expressing cell (Holland et al., 1996; Brückner et al., 1997).

VAB-1 likely has some forward signaling functions, because missense alterations of conserved residues in the kinase domain cause partial reduction in *vab-1* function. However, none of the VAB-1 kinase alleles causes complete loss of *vab-1* function. It is possible that the weak phenotype of these mutants is due to residual kinase activity. However, the kinase subdomains deleted in *e118* mutants contain residues essential for catalytic activity (Yaciuk and Shalloway, 1986); also, lesions equivalent to those of *vab-1(e2)* and *vab-1(e116)* were found in the null alleles *sy7* and *sy5* of the *C. elegans let-23* RPTK, indicating that such mutations

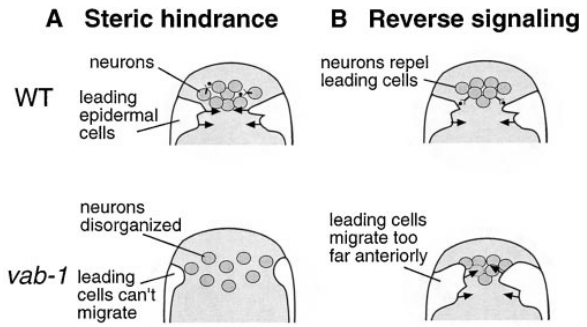

Figure 6. Two Models for the Function of VAB-1 in Epidermal Morphogenesis

See discussion for details.

cause complete loss of activity of the LET-23 kinase (Aroian et al., 1994). Thus, the VAB-1 kinase domain mutations should abolish kinase activity.

An alternative explanation for the weak phenotypes of *vab-1* kinase mutants is that VAB-1, in addition to kinase-dependent forward signaling functions, has kinase-independent reverse signaling functions. Such functions presumably require the VAB-1 extracellular domain, possibly interacting with ephrin ligands, and would explain why only mutations disrupting the VAB-1 extracellular domain would cause null phenotypes. As discussed below, VAB-1 reverse signaling could account for the nonautonomous role of *vab-1* in epidermal morphogenesis. As both weak and strong *vab-1* alleles appear to cause similar ranges of phenotypes with different penetrances, the kinase-dependent and kinase-independent functions of *vab-1* may be required for related aspects of morphogenesis.

The Role of VAB-1 in Signaling from Neurons to Epidermis during Epidermal Morphogenesis

vab-1 mutants are defective in the movements of neuroblasts that close the ventral gastrulation cleft and the movements of the epidermal leading cells that initiate epidermal enclosure. Unexpectedly, *vab-1* is not expressed in the epidermal leading cells but in neurons underlying or adjacent to the leading cells. In addition, our mosaic analysis has shown that loss of *vab-1* function in nonepidermal precursors causes epidermal morphogenetic defects. Our results suggest that a major function of *vab-1* is in neuronal cells and that the epidermal morphogenesis defects of *vab-1* mutants in part result from defects in neuronal cells. Thus, despite its similarity to receptors, VAB-1 acts in signaling rather than responding cells.

Our observations raise two questions: what signals do underlying neurons provide to migrating epidermal cells, and does VAB-1 function directly in such neuronal-to-epidermal signaling? We propose two models for this process (Figure 6). These two models are not mutually exclusive, and the phenotypes of *vab-1* mutants suggest that both models might apply. In the "steric hindrance" model (Figure 6A), VAB-1 signaling only occurs between neuronal precursors, and the epidermal defects in *vab-1* mutants are a result of defects in neuronal precursors that normally provide a permissive substrate for epidermal cell movements. Mispositioned neuronal precursors resulting from the gastrulation cleft defects seen in *vab-1* mutant embryos could interfere with normal epidermal migration and likely contribute to the epidermal defects seen in severely mutant *vab-1* animals (class I-III). However, we often observe defects in enclosure in the absence of obvious defects in cleft closure (class IV phenotype). Thus, defects in epidermal enclosure do not appear to be solely due to defects in neuroblast movements following gastrulation.

In the "reverse signal" model (Figure 6B), neurons signal directly to epidermal cells, potentially providing cues for their migration. As discussed above, VAB-1 could participate directly in such reverse signaling, analogous to that observed for vertebrate Eph receptors. Alternatively, VAB-1 could receive a signal from epidermal cells and thereby activate a second signaling pathway in the reverse direction. Two observations further suggest that VAB-1–expressing cells might provide an inhibitory signal to epidermal cells. First, in wild-type embryos the leading cells migrate posteriorly and adjacently to VAB-1–expressing cells (Figures 4B–4E). Second, in some *vab-1* mutant embryos the leading cells migrate anteriorly to their normal positions, possibly a result of a lack of anterior repulsive cues. Identification and localization of ligands for VAB-1 is necessary to distinguish between these two models for VAB-1.

Our genetic analysis of *vab-1* has shown that the null phenotype of *vab-1* is a variable defect in epidermal morphogenesis. As a small percentage of *vab-1* null mutants develop into apparently normal adults, *vab-1* function is not essential. *vab-1* signaling may be partly redundant with other signaling pathways, as found for some vertebrate Eph receptors (Orioli et al., 1996), although no additional Eph receptors have yet been identified in the *C. elegans* genomic sequence.

Eph Signaling in Vertebrate Morphogenesis

Signaling via Eph receptors and ligands has been implicated in axon guidance and topographic mapping (Cheng et al., 1995; Gao et al., 1996; Henkemeyer et al., 1996; Nakamoto et al., 1996). Ephrin signaling can function as a repulsive cue for axon guidance by promoting growth cone collapse (Drescher et al., 1995). Ephrin signaling has also been shown to promote axon fasciculation (Winslow et al., 1995), formation of rhombomere boundaries (Xu et al., 1995), and to inhibit cell–cell adhesion (Winning et al., 1996). A common feature of Eph-mediated signaling is thus the modulation of cell shape and cell adhesion, processes critical to epithelial morphogenesis.

The expression patterns of many vertebrate Eph receptors suggest they may be functioning in epithelial morphogenesis. For example, EphB2/Nuk is expressed in midline epithelial cells of the palatal shelves as they begin to fuse in the midline. Mice lacking both the EphB2 and EphB3/Sek4 receptors have cleft palates as a result of failure in closure of the secondary palate, possibly due to defective epithelial morphogenesis (Orioli et al., 1996). Many other Eph receptors are expressed in epithelial or endothelial organs undergoing morphogenesis, such as lung, heart (Ruiz et al., 1994), or in migrating cells (Brändli and Kirschner, 1995). Determining the

roles of vertebrate Eph receptors in these processes may be complicated by redundancy between members of this gene family; for example, EphA2/Eck is specifically expressed during mouse gastrulation (Ruiz and Robertson, 1994), yet Eck mutant mice show no discernible phenotype (Chen et al., 1996). *vab-1* may provide a relatively simple model for understanding the functions of Eph receptors in these aspects of vertebrate morphogenesis.

Experimental Procedures

Genetic Analysis of *vab-1*

C. elegans strains were cultured using standard methods (Brenner, 1974). Mutations used were as follows: LGI, *unc-29(e1072)*; LG II, *lin-31(n301)*, *hlh-1(cc450)*, *dpy-25(e817sd)*, and *tra-2(q122dm)* (Schedl and Kimble, 1988); LGIII, *ncl-1(e1865)*; and LGX, *lin-15(n765ts)*. Rearrangements used were *ccDf4*II and *maDf4*II. Mutations are described in Hodgkin (1997) or in references above.

vab-1 alleles were isolated in general screens for visible mutations by S. Brenner (*e2*, *e116*, *e118*, *e200*, *e699*, *e721*, *e856*, and *e1059*), J. Lewis (*e1029*), J. Hodgkin (*e1063*), A. Fire (*e2027*), E. Lambie (*dx14, dx31*), M. Zhen (*ju8*), D. Ostertag (*ju22, ju63*), and D. Greenstein (*tn2*). All alleles were EMS-induced except *dx14* and *dx31*, which were UV-induced, and *e2027*, which arose spontaneously. All mutations fail to complement *vab-1(e2)*. Map data showing that *vab-1* lies close to the right of *hlh-1* are available from the Caenorhabditis Genetics Center.

Phenotypic Analysis

We determined the penetrance of *vab-1* mutant phenotypes by picking L4 animals from homozygous strains to separate plates, allowing them to self, and transferring them every 24 hr. Eggs unhatched after 24 hr were scored as embryonic arrest. Larvae that failed to develop into adults after 48 hr were scored as larval arrest. Any morphological abnormality of the head region was scored as abnormal. At least 500 individuals were scored for each genotype.

We determined the stages at which *vab-1* embryos arrest by following the development of *vab-1* embryos using Nomarski microscopy. Embryos were followed from comma stage or before until either development arrested or the embryo hatched. To generate embryos heterozygous for *vab-1* alleles and the deficiency *ccDf4*, we mated males carrying the dominant feminizing mutation *tra-2(q122)* with *ccDf4/dpy-25* hermaphrodites; non-Dpy cross progeny are *ccDf4/tra-2* females. These females were mated with *vab-1*/+ males. One quarter of the F_1 animals from this cross will be of genotype *vab-1/ccDf4*.

To generate animals transheterozygous for deficiencies that uncover *vab-1*, *tra-2(q122)* males were mated with *ccDf4/dpy-25* hermaphrodites and *maDf4/dpy-25* hermaphrodites in separate crosses. Non-Dpy female cross progeny (genotype *ccDf4/q122*) from the first cross were mated with non-Dpy male cross progeny (genotype *maDf4/q122*) from the second cross. One quarter of the progeny of this cross were *ccDf4/maDf4* heterozygotes.

Analysis of Cell Movements by Time-Lapse Nomarski Microscopy

Four-dimensional microscopy was used to record and follow cell movements as described (Williams-Masson et al., 1997). To generate the movies analyzed, 30 focal planes 0.5 μm apart were recorded every 60 s. A total of 58 *vab-1(e2027)* embryos were recorded from early gastrulation until they had reached a terminal phenotype. We found that some *vab-1* embryos develop more slowly than wild-type embryos following gastrulation and morphogenesis. Wild-type embryos took 320 min to develop from the eight-cell stage to the beginning of elongation. *vab-1* embryos took up to 55 min longer to develop to this stage, with the developmental delay correlating with the severity of the morphogenetic defects.

Transformation Rescue of *vab-1*

vab-1(e2027) animals were injected with cosmid M03A1 (15 μg/ml) and the plasmid pRF4 (50 μg/ml), which confers a dominant Roller (Rol) phenotype (Mello et al., 1991). Transgenic lines carrying pRF4 and M03A1 in extrachromosomal arrays were established and scored for rescue of the Vab-1 phenotypes. Five of six lines showed rescue of the *vab-1* embryonic lethality and head morphology defects (2.8% of Rols were Vab in rescued lines), compared with 0/2 control lines bearing pRF4 alone (86.5% of Rols were Vab).

Analysis of *vab-1* cDNA Sequence

cDNAs from the *vab-1* locus had been isolated in a genome-wide EST project (Y. Kohara, personal communication). The longest cDNA clone, yk18c8, contains a 2992 bp insert that we sequenced, corresponding to bases 700–3962 of the composite *vab-1* cDNA. We determined the 5′ end (bases 1–699) of the *vab-1* transcript in RT-PCR experiments; RT-PCR using the SL1 *trans*-spliced leader sequence as upstream primer (Krause and Hirsh, 1987) generated products, indicating that the *vab-1* message is *trans*-spliced to SL1. The *vab-1* cDNA sequence is 3962 bp in length, consistent with the 4 kb band observed on Northern blots (data not shown), including an SL1 *trans*-spliced leader, an 89 bp 5′ UTR, a 3354 bp open reading frame, and a 458 bp 3′ UTR. No evidence was found for alternative *vab-1* transcripts either by Northern blot or RT-PCR experiments.

Determination of Mutant DNA Sequences

We determined the sequences of genomic DNAs from *vab-1* mutants as described previously (Chisholm and Horvitz, 1995). *vab-1* exons and splice sites were amplified from all *vab-1* mutants (except the deletion alleles *dx14*, *dx31*, *e118*, and *e2027*) and PCR products sequenced using ^{33}P labeled primers and the fmol kit (Promega). All mutations were confirmed on both strands and in independent PCRs. The molecular lesions of two *vab-1* mutations (*e721* and *e1029*) have not yet been found. Sequences of primers used are available upon request.

The *vab-1* alleles *dx14* and *dx31* result from rearrangements, based on Southern blot analysis of mutant genomic DNA (data not shown). *dx31* causes a deletion of at least 7 kb, removing exons 1-4. *dx14* appears to be a complex rearrangement, resulting in an approximately 2 kb deletion that deletes exon 4 and the first half of exon 5.

vab-1::GFP Reporter Constructs

The VAB-1::GFP construct pCZ55 used for expression studies is a translational fusion of GFP to a *vab-1* minigene and contains 4.2 kb of genomic sequence 5′ to the *vab-1* start codon, exons 1-5 (to the SmaI site in exon 5) as genomic DNA, exons 6-10 as cDNA, GFP inserted in frame at the XhoI site near the VAB-1 N terminus, the *vab-1* 3′ UTR, and 0.4 kb of genomic DNA 3′ to the polyadenylation site.

Transgenic lines were generated by transformation of *vab-1(e2027)*; *lin-15* animals with pCZ55 and the *lin-15* rescuing plasmid pLin-15EK (Clark et al., 1994); four independent chromosomal integrants (*juIs24*, *juIs31*, *juIs32*, and *juIs33*) were identified following X-ray mutagenesis. Expression was analyzed in the strain CZ723 of genotype *vab-1(e2027)*; *lin-15(n765)*; *juIs24(vab-1*::GFP; *lin-15*[+]) by staining fixed transgenic animals with anti-GFP antibodies. Embryos were fixed in 1% paraformaldehyde and incubated with anti-GFP polyclonal antisera (Clontech) at 1:100 to 1:500 dilution and with MH27 monoclonal (1:1500). Staining was visualized with fluorescently conjugated secondary antibodies using a confocal microscope. VAB-1::GFP staining patterns in all four lines were indistinguishable.

Analysis of *vab-1* Genetic Mosaics

We used two approaches to identify *vab-1* mosaic animals. In both approaches we generated transgenic arrays bearing wild-type copies of *vab-1* and cell-autonomous marker genes (Herman, 1995). First, we generated strains of genotype *unc-29*; *vab-1*; *juEx(unc-29*[+] *vab-1*[+] *sur-5*-GFP) by transformation of *unc-29*; *vab-1* worms with cosmid DNAs C45G10 (*unc-29*[+] [Miller et al., 1996]), M03A1 (*vab-1*[+]) and the *sur-5*-GFP plasmid pTG96.1. *sur-5*-GFP is expressed in most somatic cell nuclei (T. Gu and M. Han, personal communication) and is a cell-autonomous marker for the array; *unc-29*(+) is required in body muscles (derived from P_1) (Miller et al.,

1996). From such strains, three Unc non-Vab mosaics were identified and found to have lost the array in P_1. We then screened for Vab non-Unc animals (putative mosaics with losses in AB). Twenty-three of such animals were found that had patterns of *sur-5*-GFP interpretable as resulting from losses of the array within AB.

We used the cell-autonomous marker *ncl-1* (Hedgecock and Herman, 1995) in additional mosaic analysis experiments. We generated the strain CZ712 *vab-1*; *ncl-1*; *juEx39*(*vab-1*[+] *ncl-1*[+] *rol-6*[dm]) by transformation with cosmids containing the wild-type copies of *vab-1* (M03A1), *ncl-1*(C33D3 [Miller et al., 1996]) and pRF4. Expression of *rol-6(dm)* in cells contributing to the epidermal syncytium hyp7 confers a Rol phenotype. Transgenic animals are thus Rol non-Vab non-Ncl. We screened CZ712 Rols for rare Rol Vab animals, predicted to be mosaics in which the array had been lost from a subset of hyp7 precursors. We found 15 mosaics with patterns of Ncl cells resulting from single losses of the array. Ncl cannot be scored in syncytial nuclei unless all precursors of the syncytium have lost the array, so we assessed the loss point by scoring identifiable cell nuclei, as described (Clark et al., 1993).

Of the 15 Rol Vab mosaic animals, 4 had losses in the nonepidermal precursors ABprp and ABplp. As these mosaics had been selected on the basis of their Vab phenotype, it was possible that they were rare double loss mosaics in which the Vab phenotype was due to loss of the array in epidermal cells (which we could not directly score), rather than the observed loss in nonepidermal precursors. To address this caveat we screened CZ712 Rols directly for mosaicism of the Ncl marker. From 800 Rols screened we identified 42 animals with mosaic Ncl expression. Of these 42 mosaics, 8 had lost the array in nonepidermal precursors, of which 6 were Vab, and 13 had lost the array in head epidermal precursors, of which 1 was Vab. Thus, loss of *vab-1* function in nonepidermal precursors can frequently cause Vab phenotypes.

Acknowledgments

We thank the colleagues above for *vab-1* mutants, the *C. elegans* genome consortium for cosmids and sequence data, and Yuji Kohara for *vab-1* cDNAs. We thank Chuck Wilson for use of his oligo synthesizer, Dawne Shelton for oligo synthesis, Bill Sullivan for help with confocal microscopy, and Doug Kellogg for the motherlode. We thank Yishi Jin for extensive advice, Mei Zhen for invaluable help, Derek Ostertag and Inessa Grinberg for help with allele sequencing, Andy Fire for advice, Jeff Simske for help with phalloidin staining, and members of the Chisholm, Jin, and Hardin labs for discussions. We thank Cori Bargmann, Gian Garriga, Ian Chin-Sang, and John Tamkun for comments on the manuscript. Some strains were provided by the Caenorhabditis Genetics Center, which is funded by the National Institutes of Health (NIH). K. S. was supported by an NIH training grant. Part of this work was supported by grants to J. H. (NSF IBN9357246 and a Lucille P. Markey Scholar Award) and by a grant to A. D. C. (NIH GM54657). A. D. C. is an Alfred P. Sloan Research Fellow.

Received December 17, 1997; revised January 29, 1998.

References

Aroian, R.V., Lesa, G.M., and Sternberg, P.W. (1994). Mutations in the *Caenorhabditis elegans let-23* EGFR-like gene define elements important for cell-type specificity and function. EMBO J. *13*, 360–366.

Bard, J. (1992). Morphogenesis. (Cambridge, England: Cambridge University Press).

Brändli, A.W., and Kirschner, M.W. (1995). Molecular cloning of tyrosine kinases in the early Xenopus embryo: identification of Eck-related genes expressed in cranial neural crest cells of the second hyoid arch. Dev. Dynam. *203*, 119–140.

Brenner, S. (1974). The genetics of *Caenorhabditis elegans*. Genetics *77*, 71–94.

Brückner, K., Pasquale, E.B., and Klein, R. (1997). Tyrosine phosphorylation of transmembrane ligands for Eph receptors. Science *275*, 1640–1643.

Chen, J., Nachabah, A., Scherer, C.P.G., Reith, A., Bronson, R., and Ruley, H.E. (1996). Germ-line inactivation of the murine Eck receptor tyrosine kinase by gene trap retroviral insertion. Oncogene *12*, 979–988.

Cheng, H.-J., Nakamoto, M., Bergemann, A.D., and Flanagan, J.G. (1995). Complementary gradients in expression and binding of ELF-1 and Mek4 in development of the topographic retinotectal projection map. Cell *82*, 371–381.

Chisholm, A.D., and Horvitz, H.R. (1995). Patterning of the head region of *Caenorhabditis elegans* by the *Pax-6* family member *vab-3*. Nature *377*, 52–55.

Clark, S.G., Chisholm, A.D., and Horvitz, H.R. (1993). Control of cell fates in the central body region of *C. elegans* by the homeobox gene *lin-39*. Cell *74*, 43–55.

Clark, S.G., Lu, X., and Horvitz, H.R. (1994). The *Caenorhabditis elegans* locus *lin-15*, a negative regulator of a tyrosine kinase signaling pathway, encodes two different proteins. Genetics *137*, 987–997.

Connor, R.J., and Pasquale, E.B. (1995). Genomic organization and alternatively processed forms of Cek5, a receptor protein-tyrosine kinase of the Eph subfamily. Oncogene *11*, 2429–2438.

Costa, M., Wilson, E.T., and Wieschaus, E. (1994). A putative cell signal encoded by the folded gastrulation gene coordinates cell shape changes during *Drosophila* gastrulation. Cell *76*, 1075–1089.

Drescher, U., Kremoser, C., Handwerker, C., Löschinger, J., Noda, M., and Bonhoeffer, F. (1995). In vitro guidance of retinal ganglion cell axons by RAGS, a 25 kDa tectal protein related to ligands for the eph receptor tyrosine kinases. Cell *82*, 359–370.

Eph Nomenclature Committee (1997). Unified nomenclature for Eph family receptors and their ligands, the ephrins. Cell *90*, 403–404.

Fox, G.M., Holst, P.L., Chute, H.T., Lindberg, R.A., Janssen, A.M., Basu, R., and Welcher, A.A. (1995). cDNA cloning and tissue distribution of five human EPH-like receptor protein-tyrosine kinases. Oncogene *10*, 897–905.

Gale, N.W., Holland, S.J., Valenzuela, D.M., Flenniken, A., Pan, L., Ryan, T.E., Henkemeyer, M., Strebhardt, K., Hirai, H., Wilkinson, D.G., et al. (1996). Eph receptors and ligands comprise two major specificity subclasses and are reciprocally compartmentalized during embryogenesis. Neuron *17*, 9–19.

Gao, P.-P., Zhang, J.-H., Yokoyama, M., Racey, B., Dreyfuss, C.F., Black, I.B., and Zhou, R. (1996). Regulation of topographic projection in the brain: Elf-1 in the hippocamposeptal system. Proc. Natl. Acad. Sci. USA *93*, 11161–11166.

Glise, B., Bourbon, H., and Noselli, S. (1995). *hemipterous* encodes a novel *Drosophila* MAP kinase, required for epithelial cell sheet movement. Cell *83*, 451–461.

Hedgecock, E.M., and Herman, R.K. (1995). The *ncl-1* gene and genetic mosaics of *Caenorhabditis elegans*. Genetics *141*, 989–1006.

Henkemeyer, M., Orioli, D., Henderson, J.D., Saxton, T.M., Roder, J., Pawson, T., and Klein, R. (1996). Nuk controls pathfinding of commissural axons in the mammalian central nervous system. Cell *86*, 35–46.

Herman, R.K. (1995). Mosaic analysis. In Caenorhabditis elegans: Modern Biological Analysis of an Organism, H.F. Epstein and D.C. Shakes, eds. (San Diego, California: Academic Press), pp. 123–146.

Hirai, H., Maru, Y., Hagiwara, K., Nishida, J., and Takaku, F. (1987). A novel putative tyrosine kinase receptor encoded by the *eph* gene. Science *238*, 1717–1720.

Hodgkin, J.A. (1997). Appendix 1: genetics. In *C. elegans* II, D.L. Riddle, T. Blumenthal, B.J. Meyer, and J.R. Priess, eds. (Cold Spring Harbor, New York: Cold Spring Harbor), pp. 881–1048.

Holland, S.J., Gale, N.W., Mbalamu, G., Yancopoulos, G.D., Henkemeyer, M., and Pawson, T. (1996). Bidirectional signaling through the EPH-family receptor Nuk and its transmembrane ligands. Nature *383*, 722–725.

Hubbard, S.R., Wei, L., Ellis, L., and Hendrickson, W.A. (1994). Crystal structure of the tyrosine kinase domain of the human insulin receptor. Nature *372*, 746–754.

Knust, E. (1997). Drosophila morphogenesis: movements behind the edge. Curr. Biol. *7*, R558-R561.

Krause, M., and Hirsh, D. (1987). A trans-spliced leader sequence on actin mRNA in *C. elegans*. Cell *49*, 753–761.

Labrador, J.P., Brambilla, R., and Klein, R. (1997). The N-terminal globular domain of Eph receptors is sufficient for ligand binding and receptor signaling. EMBO J. *16*, 3889–3897.

Maisonpierre, P.C., Barrezueta, N.X., and Yancopoulos, G.D. (1993). Ehk-1 and Ehk-2: two novel members of the Eph receptor-like tyrosine kinase family with distinctive structures and neuronal expression. Oncogene *8*, 3277–3288.

Mello, C.C., Kramer, J.M., Stinchcomb, D., and Ambros, V. (1991). Efficient gene transfer in *C. elegans*: extrachromosomal maintenance and integration of transforming sequences. EMBO J. *10*, 3959–3970.

Miller, L.M., Waring, D.A., and Kim, S.K. (1996). Mosaic analysis using a *ncl-1*(+) extrachromosomal array reveals that *lin-31* acts in the Pn.p cells during *Caenorhabditis elegans* vulval development. Genetics *143*, 1181–1191.

Nakamoto, M., Cheng, H.-J., Friedman, G.C., Mclaughlin, T., Hansen, M.J., Yoon, C.H., O'Leary, D.D.M., and Flanagan, J.G. (1996). Topographically specific effects of ELF-1 on retinal axon guidance in vitro and retinal axon mapping in vivo. Cell *86*, 755–766.

O'Bryan, J.P., Frye, R.A., Cogswell, P.C., Neubauer, A., Kitch, B., Prokop, C., Espinosa, R., III., Le Beau, M.M., Earp, H.S., and Liu, E.T. (1991). *axl*, a transforming gene isolated from primary human myeloid Leukemia cells, encodes a novel receptor tyrosine kinase. Mol. Cell Biol. *11*, 5016–5031.

Orioli, D., and Klein, R. (1997). The Eph receptor family: axonal guidance by contact repulsion. Trends Genet. *13*, 354–359.

Orioli, D., Henkemeyer, M., Lemke, G., Klein, R., and Pawson, T. (1996). Sek4 and Nuk receptors cooperate in guidance of commissural axons and in palate formation. EMBO J. *15*, 6035–6049.

Parks, S., and Wieschaus, E. (1991). The *Drosophila* gastrulation gene *concertina* encodes a Gα-like protein. Cell *64*, 447–458.

Pasquale, E.B. (1991). Identification of chicken embryo kinase 5, a developmentally regulated receptor-type tyrosine kinase of the Eph family. Cell Reg. *2*, 523–534.

Priess, J., and Hirsh, D. (1986). *Caenorhabditis elegans* morphogenesis: the role of the cytoskeleton in the elongation of the embryo. Dev. Biol. *117*, 156–173.

Riesgo-Escovar, J.R., Jenni, M., Fritz, A., and Hafen, E. (1996). The Drosophila Jun-N-terminal kinase is required for cell morphogenesis but not for DJun-dependent cell fate specification in the eye. Genes Dev. *10*, 2759–2768.

Ruiz, J.C., and Robertson, E.J. (1994). The expression of the receptor-protein tyrosine kinase gene, *eck*, is highly restricted during early mouse development. Mech. Dev. *46*, 87–100.

Ruiz, J.C., Conlon, F.L., and Robertson, E.J. (1994). Identification of novel protein kinases expressed in the myocardium of the developing mouse heart. Mech. Dev. *48*, 153–164.

Schedl, T., and Kimble, J. (1988). *fog-2*, a germ-line-specific sex determining gene required for hermaphrodite spermatogenesis in *Caenorhabditis elegans*. Genetics *119*, 43–61.

Sluss, H.K., Han, Z., Barrett, T., Davis, R.J., and Ip, Y.T. (1996). A JNK signal transduction pathway that mediates morphogenesis and an immune response in Drosophila. Genes Dev. *10*, 2745–2758.

Sulston, J.E., Schierenberg, E., White, J.G., and Thomson, J.N. (1983). The embryonic cell lineage of the nematode *Caenorhabditis elegans*. Dev. Biol. *100*, 64–119.

Wicks, I.P., Wilkinson, D., Salvaris, E., and Boyd, A.W. (1992). Molecular cloning of *HEK*, the gene encoding a receptor tyrosine kinase expressed by human lymphoid tumor cell lines. Proc. Natl. Acad. Sci. USA *89*, 1611–1615.

Williams-Masson, E.M., Malik, A.N., and Hardin, J. (1997). An actin-mediated two-step mechanism is required for ventral enclosure of the *C. elegans* hypodermis. Development *124*, 2889–2901.

Winning, R.S., Scales, J.B., and Sargent, T.D. (1996). Disruption of cell adhesion in *Xenopus* embryos by Pagliaccio, an Eph-class receptor tyrosine kinase. Dev. Biol. *179*, 309–319.

Winslow, J.W., Moran, P., Shih, A., Valverde, J., Yuan, J.Q., Beck, K.D., Wong, S.C., Tsai, S.P., Goddard, A., Henzel, W.J., et al. (1995). Cloning of AL-1, a ligand for an Eph-related tyrosine kinase receptor involved in axon bundle formation. Neuron *14*, 973–981.

Xu, Q., Alldus, G., Holder, N., and Wilkinson, D.G. (1995). Expression of truncated *Sek-1* receptor tyrosine kinase disrupts the segmental restriction of gene expression in the *Xenopus* and zebrafish hindbrain. Development *121*, 4005–4016.

Yaciuk, P., and Shalloway, D. (1986). Features of the $pp60^{v\text{-}src}$ carboxyl terminus that are required for transformation. Mol. Cell. Biol. *6*, 2807–2819.

Genbank Accession Number

The Genbank accession number for the *vab-1* cDNA sequence is AF040269.